



INTRACOMPONENTAL AERODYNAMIC INTERACTION IN CENTRIFUGAL COMPRESSOR

Basharat Salim¹

1: Associate Professor, Department of Mechanical Engineering, King Saud University, Kingdom of Saudi Arabia

E-mail: basharat@ksu.edu.sa

ABSTRACT

This paper is an attempt to present some of the aerodynamic interactions between stationary components and rotating impeller of a centrifugal compressor. The study involved three types of inlet shapes and five types of diffuser configurations fitted to the same radial impeller with stationary shroud, volute casing and exit duct. The investigation included full flow range of these systems using traverses of three hole probe and static pressure measurements along the diffuser walls as well as diffuser blade surfaces. The results depict that the inlet duct shape, diffuser type and shape effect the wall static pressure rise both in vaneless and vaned configurations. The vane surface pressure is grossly affected by diffuser shape and to some extent by inlet duct. It is also evident from the study that aerodynamics with in the impeller is effected by the geometries of the upstream and downstream components due to the intracomponental aerodynamic interaction amongst these with the impeller.

Keywords: *Aerodynamics, centrifugal compressor, turbomachines; diffuser, impeller*

1. INTRODUCTION

The impeller of a centrifugal compressor transfers the mechanical energy of the rotating shaft into the energy of the fluid by energy exchange between the fluid and the rotating blades. The impeller of a centrifugal compressor behaves as an accelerating diffuser in the sense that it increases both the static pressure of the flowing fluid and its kinetic energy. The kinetic energy is transformed into static pressure rise in the following stationary diffuser passages either purely as a result of area enlargement as in case of vaneless diffuser or due to directional diffusion as achieved in vaned diffuser. The overall performance characteristics of a compressor comprise of the summation of characteristics of both that of the impeller and the diffuser. The shape and size of the stationary components have been found [Agarwal et al., 1994] to influence these characteristics. Many investigators, Grietzer (1981), Inoue and Cumpsty (1984), Roger (1977), Rodger (1991), Aungier (1995), Kim, Y.et.al (2001) and Salim et al. (1989), have found that stationary components of the compressor not only change the pressure characteristics of the compressor but also influence the stability of these pumping systems. Salim et al. (1990) have explained the flow details at the inlet of impeller, exit of impeller and downstream of impeller in great details. This investigation points to the effect of stationary components of compressor on its performance parameters.

2. TESTING CONFIGURATION

Nine configurations of a centrifugal compressor were tested in this study. The basic testing facility is shown in Fig. 1. The impeller, volute casing and the exit system of these configurations was the same. Impeller had 19 radial tipped blades with outlet angle of 90^0 with respect to tangential direction, tip diameter of 508 mm and diameter ratio of 0.592. The tip blade height of these blades was about 7% of the impeller exit diameter. The impeller had a matching inducer at its inlet with an inlet angle of 10^0 with respect to tangential direction. Three configurations used vaneless diffuser, of diameter ratio 2, down stream of impeller. These vaneless configurations used three types of inlet ducts as shown in Fig. 2 and were termed as CV1, CV2 and CV3. Three counter parts of these vaneless configurations were the ones with vaned diffusers and were named as CD1, CD2 and CD3. The vanes of these configurations were double profiled with a log spiral at the inlet and a straight portion beyond the throat. In all eighteen vanes were used in vaned configurations with their leading edge at about a distance of 10% of impeller tip diameter downstream of impeller. The vane inlet angle of these configurations was 16 degrees with the tangential direction. It may be mentioned here that the mean exit angle of CV2 configuration was 16 degrees from tangential direction. Three more configurations were derived from CD2 configuration by changing the vane inlet angle of these configurations to 12 degree for CD4, 20 degrees for CD5 configuration and 24 degrees for CD6 configuration. The impeller was connected to a motor through a gear system which allowed variation in the rotational speed of the impeller. The measurements were taken at a constant speed of 3000 rpm. Investigations were carried out by using 3 hole probe, total pressure probe, wall tapings and the read out devices were inclined manometers of high

degree of readability and accuracy and digital micro monometers. The pressure tubes of the 3 hole probe were fabricated from 0.8 mm steel tubings in such a manner that the flow blockage at the exit of the impeller was less than 2.5%. The uncertainty estimates of various measured flow parameters, which has been carried out by the method of Kline et al (1953) is tabulated in table 1.

3. RESULTS AND DISCUSSION

The present investigation was carried out to establish the dependence of performance of a centrifugal compressor on the geometry and shape of its stationary components. The overall performance of a compressor is usually represented by change in static pressure rise coefficient through the impeller and the stage with the flow coefficient. Other performance coefficients that are of importance are blockage at impeller exit, throat of diffuser, slip, work done factor, pressure recovery coefficient, total pressure loss coefficient, wall static pressure rise and vane static pressure rise.

Static Pressure Rise Coefficient:- The static pressure rise coefficient is obtained from the average static pressure measurements at the exit of impeller or exit of the stage. This total pressure at the inlet of impeller is subtracted from the measured value of static pressure and the result divided by the dynamic head corresponding to the impeller tip speed. The two coefficients thus obtained are plotted against the flow coefficient defined by the ratio of radial velocity at the exit of impeller to the impeller tip speed. These variations have been shown for both the vaneless and vaned configurations in order to depict the effect of inlet and diffuser shapes in figures 3-5. In these figures the different curves have been numbered as cv12, cd12 etc. the first two letters show the type of diffuser used in the configuration, vaneless or vaned, third number 1 to 6 depicts the type of configuration as given earlier and the fourth number 2 or 6 depicts whether the variation is for ψ_{21} or ψ_{61} for the configuration. Fig. 3 shows the variation of static pressure rise coefficient with flow coefficient for vaneless configurations with different shapes of inlets. In these configurations even though CV3 shows both the higher values of static pressure rise coefficient and the stable flow range as compared to other two the pressure rise in the diffuser is highest for CV2. Amongst the vaned configuration, Fig. 4, the configuration CD2 shows the maximum values of ψ . The change in vane inlet angle of diffuser, Fig. 5, is observed not only to change the magnitudes of static pressure rise but also the trend of variation of this coefficient with the flow coefficient. Therefore it is evident that the shape of both the inlet duct and diffuser alter the magnitude and trends of static pressure change in the compressor. The flow range, the difference between maximum value of flow coefficient and its minimum value, and stable operating range, difference between maximum value of flow coefficient and its value corresponding to maximum value of pressure rise coefficient, are seen to be dependant on shape of inlet and type of diffuser rather than the diffuser vane inlet angle.

Mean Flow Angle at the Exit of the Impeller:-In order to have an insight into the development of flow at the exit of impeller, three hole probe traverses were carried out at the exit of

impeller at a distance of 1% of impeller radius from the exit of impeller at four traversing locations around the impeller. From these measurements an average value of flow angle was obtained, which was plotted against the flow coefficient. It may be added here that the flow angle was measured with respect to the radial location at all the location. Its variation for vaneless configurations show that the flow is more tangential for CV2 configuration than other vaneless configurations (Fig. 6). Further for all the vaneless configurations flow is more tangential at the flow rates corresponding to the peak of static pressure rise coefficients. In vaned configurations Fig. 7 CD1 shows more tangential flow as compared to the other. The change in the vane inlet angle of vaned configurations Fig. 8 makes the flow more tangential.

Performance Parameters:-The performance parameters that have been evaluated in this study are classified into two groups; Impeller performance parameters and Diffuser performance parameters. The variation of both these parameters has been carried out to show the effect of inlet duct shape both on vaneless and vaned configurations and effect of vane inlet angle for the vaned diffuser configurations.

Impeller Performance Parameters:-The impeller performance parameters That have been evaluated are slip factor, work done factor and blockage factor. Slip factor is usually defined as the ratio of actual tangential velocity at the exit of the impeller to the tip speed of the rotor. It gave an idea of the energy transfer and pressure rise capability of the impeller. This factor is used in the one-dimensional analysis of the flow through the impeller. Figs. 9 to 11 shows the variation of slip factor for all configurations tested. Form the figures it is evident that compressor configurations CV2 and CD2 show higher values of the slip factor through out the flow range for both vaneless and vaned configurations. In case of vaneless configurations slip factor is depicted to be more at around the peak of pressure rise coefficient while as for vaned configuration slip factor first decreases and then builds up again. Slip factor is seen Fig. 11 to drastically change with vane inlet angle both in terms of magnitude and the variation with the flow rate. Therefore both the shape of inlet, type and shape of diffuser affect the slip factor of a compressor.

Work done factor is another impeller performance factor used to estimate fluid power and is defined as

$$\omega_f = (U_2 * V_{t2} - U_1 * V_{t1}) / (2 * U_2^2) \quad (1)$$

The values of tip speeds at the inlet and exit of the impeller are dependent on rpm of impeller and the respective diameters whereas the tangential velocity components have been obtained from actual probe traverses at the inlet and the exit of the impeller. Fig. 12 and Fig. 13 depict the variation of work done factor for vaneless and vaned configurations with different inlet duct systems respectively. In both cases it is evident that configurations CV2 and CD2 show higher values of work done factor in vaneless and vaned configurations respectively, while as CV3 and CD3 configurations yield lower values. It may be added here that both these configurations had same form of inlet shape. Further the work done factor also changes with

the flow rates as is expected. The change in the vane inlet angle Fig. 14 alters both the values the trends of the work done factor for the vaned diffuser configuration.

Blockage factor is the most important factors of the impeller as it dictates the flow behaviour in the compressor. This factor can easily quantified either from velocity traverses as reported by Yoshingha et al. (1980) or by pressure measurements as done by Clements and Arth (1987). The blockage factor in this report is evaluated by the method given by Yoshingha et al. (1987). Blockage factor is a measure of boundary layer growth and flow distortion. The vaneless configurations show, Fig.15, a growth of blockage factor up to $\phi = 0.182$ followed by a decrease in blockage factor. Blockage is more for configuration with small length of inlet duct where as lengthiest inlet duct produces lowest blockage. A similar trend is also depicted in Fig.16 by the vaned configuration. The variation of blockage with the inlet vane angle, Fig. 17, shows a decreasing trend of blockage factor with flow rates.

Diffuser Performance Parameter:- The diffuser performance parameters that have been investigated are diffuser throat blockage factor ,wall static pressure rise, vane surface static pressure, Static pressure recovery coefficient and total pressure loss coefficient.

The Flow pattern in a diffuser is greatly influenced by the presence of the bounding (hub and shroud) walls. The flow behaviour around these surfaces complicates the whole flow picture in the diffuser. The wall static pressure readings were taken along the three radial lines from impeller exit to diffuser exit in case of vaneless diffuser configuration whereas the same were measured from diffuser inlet to diffuser exit in case of vaned configurations. The maximum value of wall static pressure thus measured was nondimensionalised by subtracting it from the static pressure at the impeller exit and dividing the result by the dynamic pressure at the exit of the impeller. Fig. 18 and 19 show the variation of C_{pw} for vaneless and vaned diffuser configurations with different shapes of inlet duct. For vaneless configuration it is noted that the configurations CV2 shows higher values of C_{pw} whereas in case of vaned configuration CD3 gives higher values of wall static pressure rise. Fig. 20 depicts that the wall static pressure rise coefficient increases with the vane inlet angle for the range of flow rates investigated and variation in the values of C_{pw} with the vane inlet angle are also noticed at all flow rates.

The flow field within the diffuser passage can be characterised by the variation of vane surface static pressure. This variation shows the possibility of flow separation within the cannels of diffuser passages. This flow separation then leads to performance degradation of the compressor. The vane surface static pressure was measured on a set of instrumented vanes on which static holes were drilled either on suction surface or on pressure surface of the vane. The pressure so obtained was subtracted from mass averaged value of pressure at the diffuse inlet, nondimensionalised with the dynamic pressure at the diffuser inlet. Fig. 21 shows the variation of maximum value of C_{pb} for vaned configurations with the change in the inlet duct shape. The variation depicts higher values of maximum vane static pressure coefficient for CD2 configuration and lowest values for the CD1 configuration. Amongst the configurations

with different vane inlet angles the values of maximum vane surface pressure is shown, Fig. 22, to be grossly effected by the changes in the vane inlet angle. The changes are not only in the values of the vane surface pressure but variation of C_{pb} with the flow coefficient are also seen to be grossly effected. At lower incidences the C_{pb} is seen to be increasing with flow rates whereas at higher values of flow incidences C_{pb} decreases with the flow rate.

The pressure recovery in the diffuser is caused by the deceleration of flow as a result of the enlargement of flow area. The pressure recovery results in the static pressure rise within the diffuser passages. For measuring the pressure recovery in the diffuser the static holes at the exit of different diffuser passages were measured. The mean of these values was subtracted from the mass averaged values of the static pressure at the inlet of diffuser, the result was non-dimensionalised with the dynamic head at the inlet of the diffuser. From the variation of pressure recovery coefficients it is seen the both vaneless, Fig. 23 and vaned configuration, Fig. 24 with medium size of inlet duct, CV2 and CD2, generate higher values of C_{pr} . Other shapes of inlet duct show lower values of C_{pr} for all the flow rates. Fig. 25 shows that at lower incidences of vane angle the pressure recovery decreases with the flow rate where as at higher vane angles it increases with the flow rate. Further the magnitudes of pressure recovery depict variations with the vane inlet angle throughout the flow range of the compressor.

The flow with in the diffuser takes place in presence of adverse pressure gradients along the diffuser passage. The situation results in the flow separation from the sides of the diffuser passage which generates the total pressure loss in these passages. It is usually depicted as total pressure loss coefficient which is obtained from the total pressure measurements at the exit of the diffuser passages. The mean total pressure at the exit of the passages were subtracted from the mass averaged values at impeller exit and then the result was non-dimensionalised with the dynamic head at the exit of the impeller. Variation of total pressure loss coefficient for vaneless configurations (Fig. 26) and vaned configurations. Fig. 27, with different shapes of inlet duct show the configuration with medium sizes of inlet duct, CV2 and CD2 generate less total pressure loss as compared to other duct shapes. For vaneless configurations total pressure loss coefficient decreases with the flow coefficient for all the configurations whereas for vaned configuration it shows different variations. Total pressure loss coefficient is also seen Fig. 28 to be altered by the change in the vane inlet angle both in terms of the magnitude and the variation with the flow rates.

Fig. 29 and Fig. 30 show the variation of throat blockage for the vaned configurations. The configuration with long inlet duct generates lower throat blockage where as the one with short inlet duct is seen to have higher value of throat blockage. Further in all configurations the throat blockage is seen to be decreasing with the increasing flow rates. The change of vane inlet angle, Fig. 30, shows a significant change in the throat blockage. Throat blockage increases with the increase in vane inlet angle through out the flow range of configurations

4. CONCLUSIONS

The following conclusions are drawn out of this investigation.

1. Flow range and stable operating range of a configuration depends more on the shape of inlet and type of diffuser rather than the shape of diffuser as dictated by diffuser vane inlet angle.
2. Flow angle at the exit of an impeller is more influenced by shape of diffuser than the shape of the inlet.
3. Slip factor of the impeller is effected both by the shape of the inlet duct and diffuser.
4. Medium sized inlet duct generates more work done factor, pressure recovery coefficient and lower total pressure loss coefficient.
5. Blockage decreases with the increasing flow rates.

REFERENCES

1. Agarwal, D.P., Salim, B., Singh, S.N., and Malhotra, R.C., 1994, "Effect of Inlet Duct and Diffuser on the Operating Range of Centrifugal Compressor," *ISROMAC-5*, Hawaii, USA.
2. Aungier, R.H.1995"Centrifugal Compressor Stage Preliminary Aerodynamic Design and Component Sizing>Paper 95-GT-78,ASME.Newyork,NY.
3. Clements, W.S. and Arth, D.W., 1987, "The influence of Diffuser Geometry on the Flow Range and Efficiency of a Centrifugal Compressor," *Proc.I. Mech.E*, UK, Vol. 201 pp. 145-152.
4. Greitzer, E.M., 1981 "The Stability Of Pumping Systems," *Trans. ASME Jour. of Fluids Engg.*, Vol. 103. pp. 103-242.
5. Inoue, M. and Cumpsty, N.A., 1984, "Experimental Study of Centrifugal Impeller Discharge Flow in Vaneless and Vaned Diffuser," *Trans. ASME Jour. Of Gas Turbine and Power*, Vol. 106, pp. 456-467.
6. Kim, Y., Engeda, A., Aungeir, R., Direnzi, G., 2001"The Influence of Inlet Flow Distortion on the Performance of a Centrifugal Compressor and the Development of an improved Inlet using Numerical Simulation" *Proc.I. Mech.E*, UK, Vol. 215 pp. 323-338
7. Kline, S.J. and McClintock, F.A. 1953 "Describing uncertainties in single sample experiments" *Mech. Engg.* 75:3-8.
8. Rodgers, C. 1991 "Centrifugal Compressor Inlet Guide Vanes for Increased Surge Margin" *Journal of Turbomachinery*,Vol.113,p.696, ASME, Newyork, NY
9. Roger, G., 1977, "Impeller Stalling as Influenced by Diffuser Limitations," *Trans ASME Jour. Of Fluids Engg.*, pp. 84-91.
10. Salim, B., Agarwal, D.P, Singh, S.N. and Malhotra, R.C., 1989, "Effect of Downstream Elements on the Flow at the Exit of a Centrifugal Compressor Rotor," *Jour. Aero Society of India*, 41(1), pp. 282-288.
11. Salim, B., Agarwal, D.P, Singh, S.N. and Malhotra, R.C., 1990, "Centrifugal Compressor Inlet Flow as Influenced by the Inlet System," *Jour. Inst. of Enggr. India*, paper UDC621.515.

12. Yoshinaga, Y., Gyobu, I., Mishina, H., Koseki, F. and Nishida, H., 1980, "Aerodynamic Performance of a Centrifugal Compressor with Vaned Diffuser," *Tran. ASME Jour. of Fluids Engg.*, Vol. 102, pp. 486-493.

NOTATIONS

<p>A flow area</p> <p>A_e Effective area = $(\int T_v * dA) / T_{v(\text{mean})}$</p> <p>B Blockage factor = A_e/A</p> <p>B_{fi} Blockage factor at impeller exit</p> <p>B_{ft} Blockage factor at diffuser throat</p> <p>C_{pb} Vane static pressure coefficient = $(p_b - p_3)/(P_3 - p_3)$</p> <p>C_{pr} Pressure recovery coefficient = $(p_5 - p_3)/(P_3 - p_3)$</p> <p>C_{pw} Wall static pressure coefficient = $(p_w - p_2)/(P_2 - p_2)$</p> <p>p Static pressure</p> <p>P Total pressure</p> <p>T_v Total velocity</p> <p>U Circumferential velocity</p> <p>V_r Radial velocity</p> <p>V_t Tangential velocity</p> <p>α Flow angle</p> <p>ϵ Total pressure loss coefficient = $(P_5 - p_2)/(P_2 - p_2)$</p> <p>ϕ Flow coefficient = V_{t2}/U_2</p> <p>ω_f Work done factor</p> <p>ψ Pressure rise coefficient = $(p_e - P_1)/(0.5 * \rho * U_2^2)$</p> <p>$\rho$ Density</p> <p>σ Slip factor</p>	<p>Subscripts</p> <p>1 Impeller inlet</p> <p>2 Impeller exit</p> <p>3 Diffuser inlet</p> <p>4 Diffuser throat</p> <p>5 Diffuser exit</p> <p>6 Stage exit</p> <p>b Vane static</p> <p>e exit</p> <p>w Wall static</p>
--	---

Table1

Parameter	Uncertainty estimate %
Total pressure	1
Static pressure	1
Flow angle	+ - 1 ⁰
Total velocity	1.5
Static pressure rise coefficient	0.3
Flow coefficient	0.1

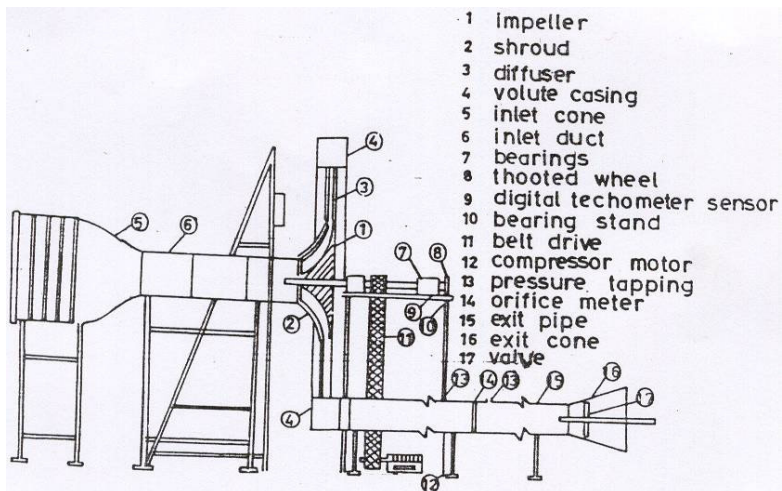


FIG.1 schematic diagram of experimental rig.

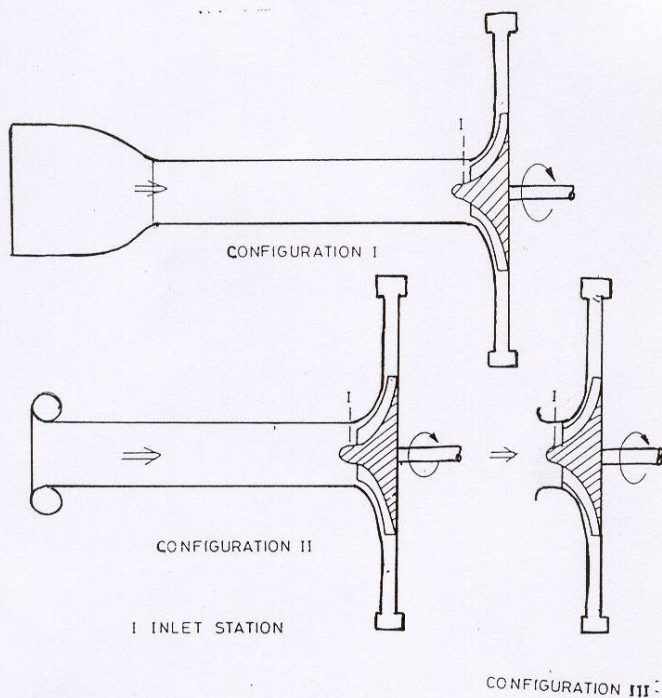


FIG. 2 INLET CONFIGURATIONS

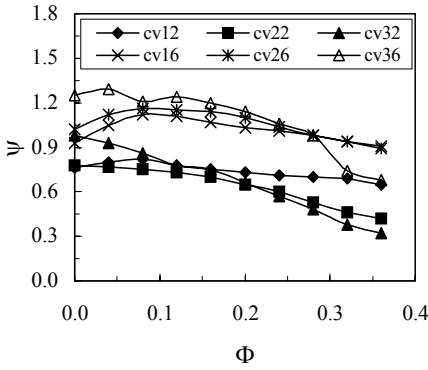


Fig. 3: Compressor characteristics of vaneless configuration

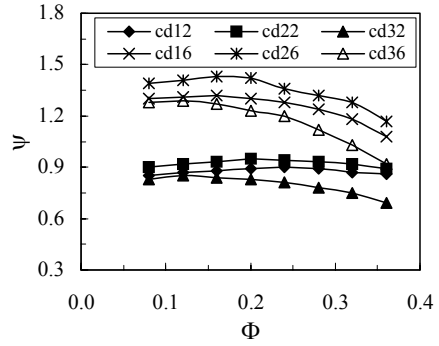


Fig. 4: Compressor characteristics of vaned configuration with different inlet shapes

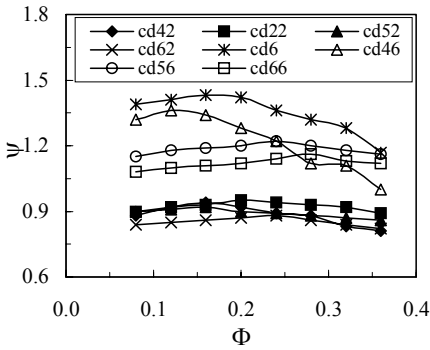


Fig. 5: Compressor characteristics of vaned configuration with different vane inlet angles

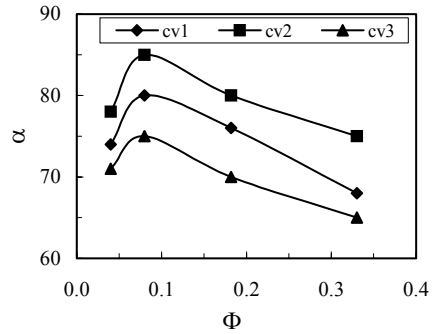


Fig. 6: Impeller exit flow angle for vaneless configuration

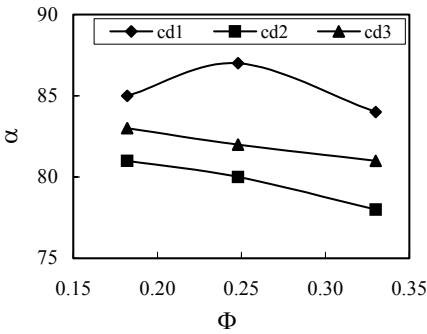


Fig. 7: Impeller exit flow angle for vaned configuration with different inlet shapes

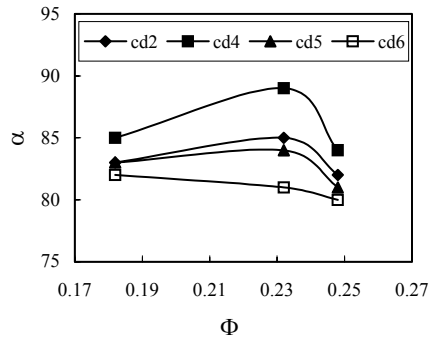


Fig. 8: Impeller exit flow angle for vaned configuration with different vane inlet angles

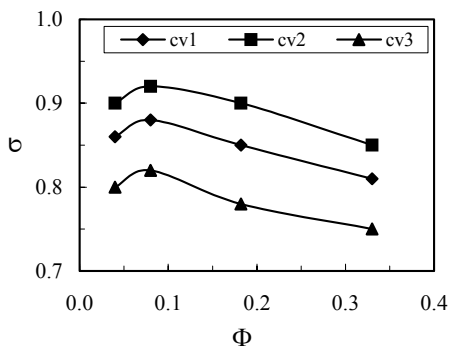


Fig. 9: Slip factor for vaneless configuration

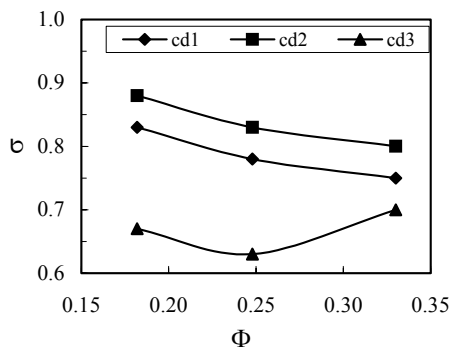


Fig. 10: Slip factor for vaned configuration with different inlet shapes

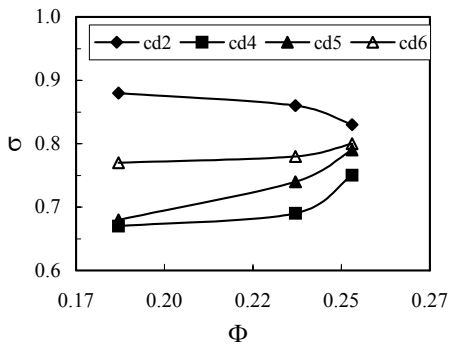


Fig. 11: Slip factor for vaned configuration with different vane inlet angles

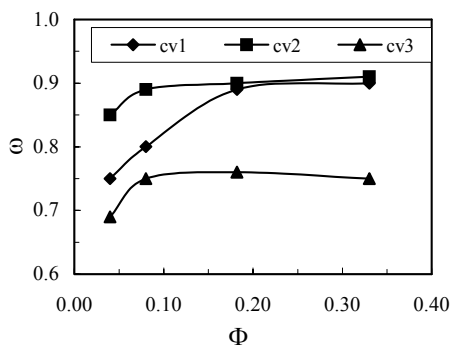


Fig. 12: Work done factor for vaneless configuration

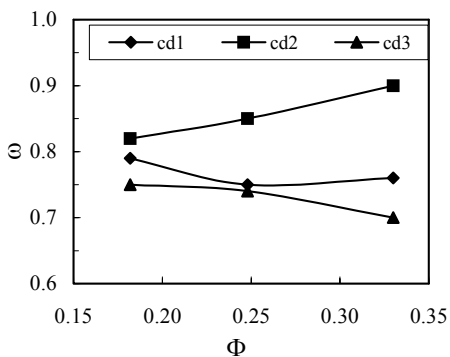


Fig. 13: Work done factor for vaned configuration with different inlet shapes

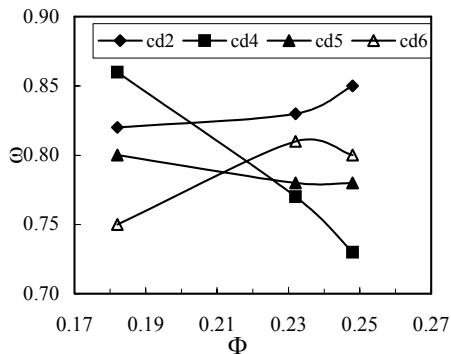


Fig. 14: Work done factor for vaned configuration with different vane inlet angles

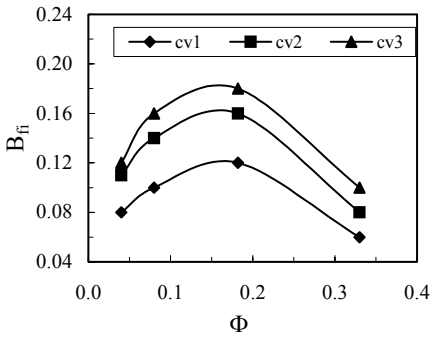


Fig. 15: Impeller exit blockage factor for vaneless configuration

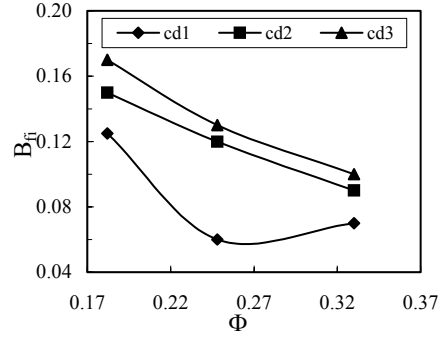


Fig. 16: Impeller exit blockage factor for vanned configuration with different inlet shapes

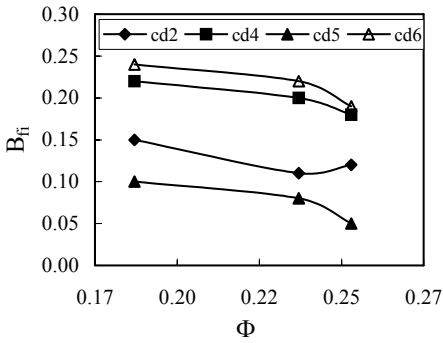


Fig. 17: Impeller exit blockage factor for vanned configuration with different vane inlet angles

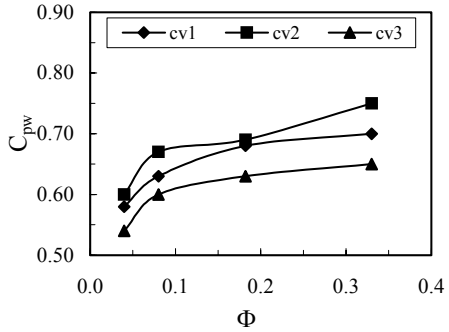


Fig. 18: Wall static pressure for vaneless configuration

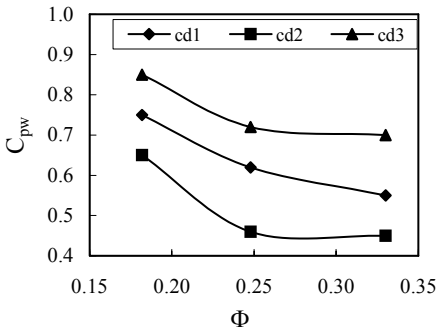


Fig. 19: Wall static pressure for vanned configuration with different inlet shapes

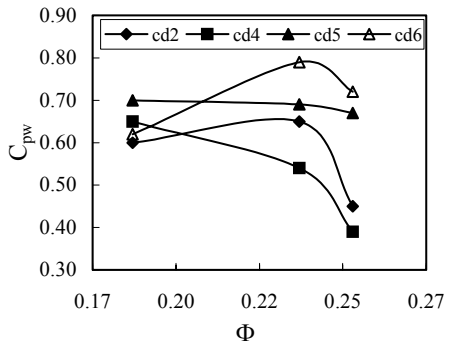


Fig. 20: Wall static pressure for vanned configuration with different vanned inlet angles

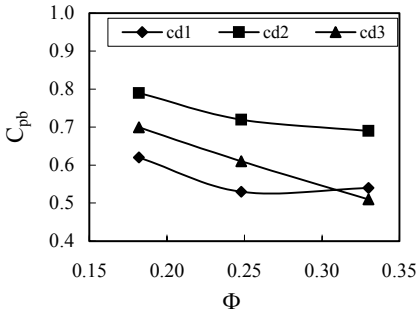


Fig. 21: Vane static pressure for vanned configuration with different inlet shapes

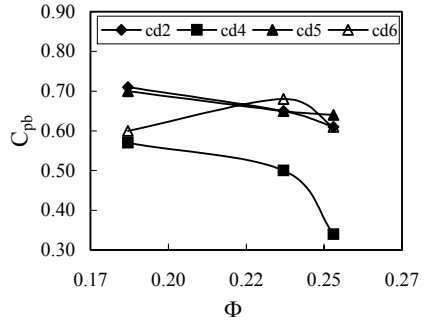


Fig. 22: Vane static pressure for vanned configuration with different vane inlet angles

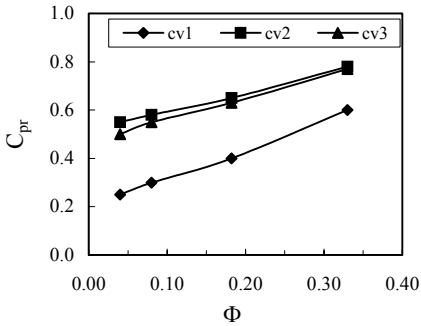


Fig. 23: Pressure recovery for vaneless configuration

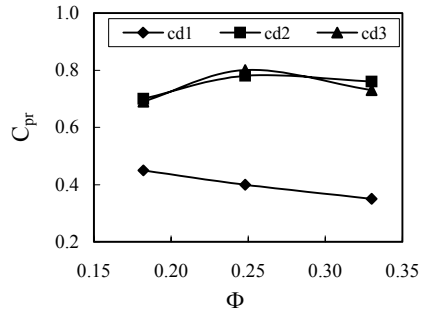


Fig. 24: Pressure recovery for vanned configuration with different inlet shapes

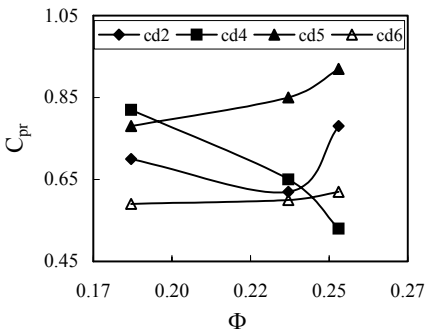


Fig. 25: Pressure recovery for vanned configuration with different vane inlet angles

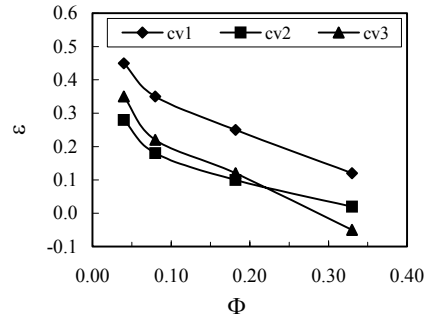


Fig. 26: Total pressure loss for vaneless configuration

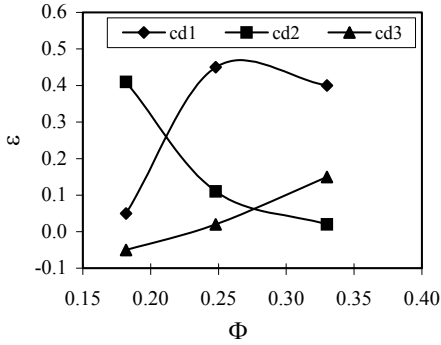


Fig. 27: Total pressure loss for vaned configuration with different inlet shapes

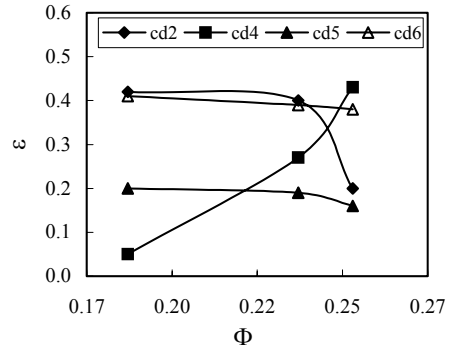


Fig. 28: Total pressure loss for vaned configuration with different vane inlet angles

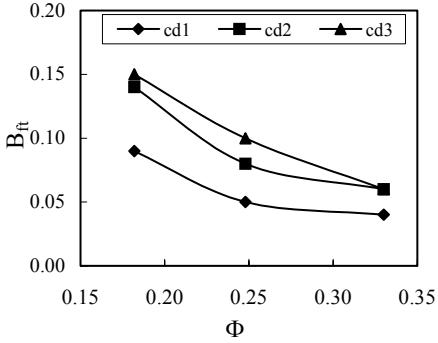


Fig. 29: Throat blockage for vaned configuration with different inlet shapes

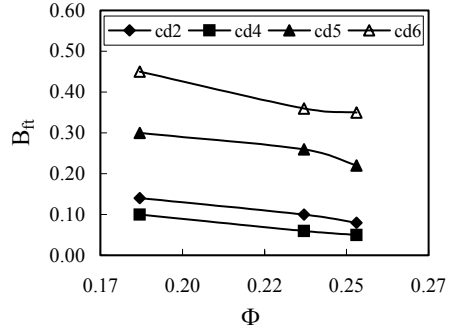


Fig. 30: Throat blockage for vaned configuration with different vane inlet angles